

Geometric Accuracy Analysis for Discrete Surface Approximation

Junfei Dai and Wei Luo

Center of Mathematics, Zhejiang Univeristy

Shing-Tung Yau

Mathematics Department, Harvard University

Xianfeng David Gu

Visual Computer Center, Stony Brook University

March 12, 2006

Abstract

In geometric modeling and processing, computer graphics, smooth surfaces are approximated by discrete triangular meshes reconstructed from sample points on the surface. A fundamental problem is to design rigorous algorithms to guarantee the geometric approximation accuracy by controlling the sampling density.

This theoretic work gives explicit formula to the bounds of Hausdorff distance, normal distance and Riemannian metric distortion between the smooth surface and the discrete mesh in terms of principle curvature and the radii of geodesic circum-circle of the triangles. These formula are applied to design sampling density.

Furthermore, we prove the meshes induced from the Delaunay triangulations of the dense samples on a smooth surface are convergent to the smooth surface under both Hausdorff distance and normal fields. The Riemannian metrics and the Laplace-Beltrami operators on the meshes are also convergent. These theoretic results lay down the foundation to guarantee the approximation accuracy of many algorithms in geometric modeling and processing.

1 Introduction

In geometric modeling and processing, computer graphics, computer vision and geometric modeling, smooth surfaces are often approximated by polygonal surfaces, which are reconstructed from a set of sample points. With the development of data acquisition techniques, such as laser scanning, CT or MRI in medical imaging, reconstructing surfaces from sample points becomes more and more important.

Different surface reconstruction algorithms have been discussed by many researchers. Hoppe et. al [HDD⁺92, EH96] represented the surface by the zero set of a signed distance function. Amenta et. al developed a series of algorithms based on voroni diagram in [ABK98, AB99, ACDL02]. Bernardini and Bajaj used α shapes for manifold sampling and reconstruction [BBX95, BB97]. Recently Ju et. al introduced the dual contour method for reconstruction [JLSW02], later Ju et. al developed an algorithm to build 3D surfaces from 2D curvature networks and applied for anatomical modeling. Floater and Reimers reconstructed surfaces based on parameterizations [FR01]. Surface reconstruction has been applied to reverse engineering [BMV01], geometric modeling [HQ04], mesh optimization and simplification [Hop96] and many other important applications.

It is a common belief that by increasing the sampling density, the reconstructed discrete mesh will approximate the smooth surface with any desired accuracy. This work aims at precisely formulating this common belief and rigorously prove it in an appropriate setting. This result will offer the theoretic guarantee for the general algorithms in geometric modeling and processing, where the measurements on smooth surface are calculated on its discrete approximations, the physical phenomena on original surface are simulated on the discrete counterpart as well.

Geometric Accuracy There are different levels of accuracy when approximating a smooth surface by discrete meshes,

1. *Topological consistency*, it requires the surface and mesh are homeomorphic to each other;
2. *Positional consistency*, measured by Hausdorff distance between the surface and the mesh;
3. *Normal consistency*, it requires the normal fields on the surface and on the mesh are close to each other.

Many previous works address the theoretic guarantee of topological consistency. Leibon et al proved that if the sample density is high enough, the smooth surface and the triangle mesh induced by the delaunay triangulation is homeomorphic in [LL00]. Amenta et. al proved similar result in [ACDL02].

In terms of positional consistency, to the best of our knowledge, the best estimation is introduced in [ACDL02]. Amenta et al invented a series of algorithms which reconstruct the meshes from sample points based on voronoi diagrams. Assume the diameter of the circum-circle of the triangles is ϵ and the normal error is small enough, the Hausdorff distance between the mesh and the surface is bounded by the ϵ^2 .

Positional consistency does not grantee the normal consistency. It is very easy to find a sequence of meshes, which converge to a smooth surface under Hausdorff distance, but the normal field does not converge. It has been shown in [HPW05], that under the assumption of convergence of Hausdorff distance, the followings are equivalent:

1. Normal field convergence
2. Area convergence,
3. Riemannian metric tensor convergence
4. Laplace-Beltrami operator convergence

In geometric modeling and processing, computer graphics, many algorithms require calculating the geodesics [SSK⁺05]. Many parameterization works require accurately approximating the Riemannian metrics [FH05], spectrum compression also needs good approximation of Laplacian-Beltrami operators [BCG05]. These important applications demand the theoretic guarantee of the normal accuracy. To the best of our knowledge, our work is the first one to bound the normal error by sampling density.

Triangulations Triangulations play vital roles in surface reconstruction. There are different ways to measure the refinement of a triangulation,

1. The bound l of the longest lengths of the edges of triangles in the mesh.
2. The bound d of the diameters of the circum-circles of triangles in the mesh.

It is obvious that the diameter bounds the edge length, but the edge length does not bound the diameter. In the following discussion, we will demonstrate that the Hausdorff distance is bounded by the square of the edge length, whereas the normal error is bounded by the diameter of the circum-circle.

In figure 1, we demonstrate a one dimensional example, where a family of curves converge to a straight line segment under Hausdorff distance. The lengths and normals do not converge.

In figure 2, we demonstrate an example, where for the same sets of sample points, the bounds of edge lengths go to zero, but the bounds of the diameters of circum-circles remain constant. Therefore, the area, the metrics on the meshes do not converge to those on the smooth surface.

Given a dense set of point samples, it is highly desirable to find a triangulation such that the circum-circles are as small as possible. For point samples on the plane, Delaunay triangulation is a good candidate for such a triangulation. Leobon generalizes Delaunay triangulation to arbitrary Riemannian manifolds []. In the following discussion, we use Delaunay triangulation to refer Delaunay triangulation on surfaces. The Delaunay triangulation is determined solely by the point samples. In the following discussion, we will show that the meshes induced by the Delaunay triangulations are convergent both under Hausdorff distance and normal distance.

In practice, there is no prior knowledge of the smooth surface, only the dense point samples are available. The connectivity induced by the surface Delaunay triangulation can be best approximated using voronoi diagram in R^3 as described in [ABK98, ACDL02]. We have not fully proven the consistency between the two triangulations.

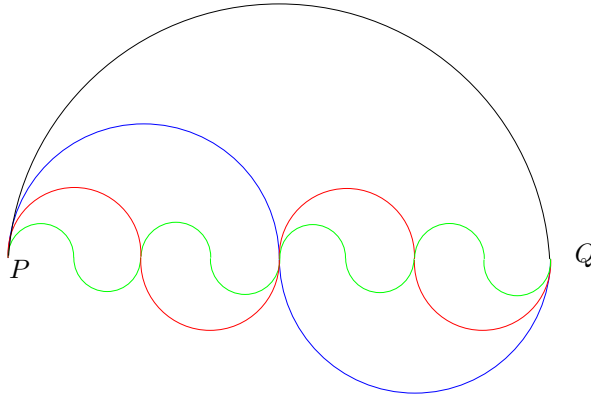


Figure 1: **Hausdorff convergence doesn't guarantee normal convergence and length convergence.** The black curve is a half circle with radius r , the blue curve is composed by two half circles with radii $\frac{r}{2}$; the red curve is composed by 4 half circles with radii $\frac{r}{4}$. A sequence of curves can be constructed, they converge to the diameter PQ under the Hausdorff distance. But the length of each of them equals to πr , which do not converge to the length of the diameter $2r$

Factors Affecting Geometric Accuracy In order to achieve bounded Hausdorff error and normal error, the following factors play crucial rules, the sampling density should be carefully designed. The major factors determine the sampling density are as followings,

- **Principle curvature** For regions with higher principle curvature, the samples should be denser.
- **Distance to medial axis** For regions closer to the medial axis, the samples should be denser to avoid topological ambiguity during the reconstruction process. It is also called local feature size.
- **Injectivity radius** Each point p on the surface M has a largest radius r , for which the geodesic disk $B(p, r)$ is an embedding disk. The injectivity radius of M is the infimum of the injectivity radii at each point. Each geodesic triangle on the surface should be contained in a geodesic disk with radius less than the injectivity radius.

These factors are not independent, but closely related. Suppose k is the bound of principle curvature on the surface, then the distance to the medial axis is no greater than $\frac{1}{k}$ as proved in [Fed59].

Comparisons to previous theoretic results Hildebrandt et.al's work [HPW05] focuses on the equivalence between convergences of polyhedral meshes under different metrics, such as Hausdorff, normal, area and Laplace-Beltrami. Assuming

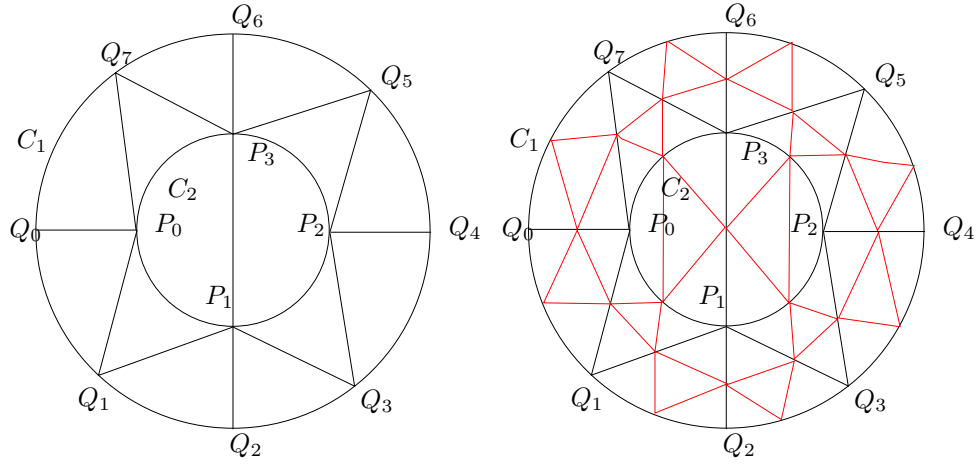


Figure 2: **Hausdorff convergence vs. normal convergence.** In the left frame, the center is the north pole of the unit sphere. C_1 is the equator, C_2 is the intersection circle between the sphere with the plane $z = \frac{1}{2}$. All the arcs Q_iQ_j and P_iQ_j are geodesics, the arcs P_iP_j are arcs along C_2 . The right frame shows one step subdivision: insert the middle points of all the arcs in the left frame, split each triangle to 4 smaller ones, such that if an edge connecting two points on C_2 , the edge is the arc on C_2 , otherwise the edge is the geodesic connecting its end points. Repeating this subdivision process to get a sequence of triangulations $\{T_n\}$, and a sequences meshes M_n induced by the triangulations. The longest edge length of T_n goes to zero, M_n converge to the hemi-sphere under Hausdorff distance. For any M_n there is one triangles f_0 adjacent to P_0 and contained in the curved triangle $P_1P_0P_3$. Because all three vertices of f_0 are on C_2 , its circumscribe circle is C_2 , the normal of f_0 is constant which differs from the normal at P_0 to the sphere. Therefore, $\{M_n\}$ doesn't converge to the sphere under normal distance.

the Hausdorff convergence and the homeomorphism between the surface and the mesh, all the error estimation is based on the homeomorphism.

Leibon et al's work [LL00] focuses on the existence of Delaunay triangulation for dense sample set. It only estimates the Riemannian metric error without considering Hausdorff error and normal error.

Amenta et al's work [ACDL02] only demonstrates the estimation of Hausdorff error under the two assumptions, first the sampling density is sufficiently high, second the normal field error is given and bounded.

Our work gives much sharper and more complete error estimations for Hausdorff error, normal error and Riemannian metric error, the only assumption is the sampling density.

The main theorem of the work is that if the sample density is ϵ , then the Hausdorff distance is no greater $4k\epsilon^2$, the normal error is no greater than $9k\epsilon$, where k is the upper bound of the principle curvature. The metric distortion is

measured by the infinitesimal length ratio, which is bounded by $1 - 4k^2\epsilon^2$ and $\frac{1+4k^2\epsilon^2}{1-9k\epsilon}$.

The paper is organized as the following, the next section 2 introduces the preliminary concepts and theorems proven in previous works; our new theoretic results are explained in details in 3. This section is the most technical part of the work, the main focus is the proofs of three major theorems; experimental results are demonstrated in section 4; Finally the paper is concluded in 5, future works will be briefly discussed.

2 Definitions and Preliminaries

In this section, we review the preliminary concepts necessary for our further theoretic arguments. We adapt the definitions from [LL00],[HPW05], [ABK98] and [ACDL02].

We assume that the surface S is closed without any boundary, at least C^2 smooth with bounded principle curvature, embedded in R^3 .

2.1 Medial axis, ϵ -sampling and Delaunay triangulation

The *medial axis* of a surface S embedded in R^3 is the closure of the set of points with more than one nearest neighbor in S . The *local feature size* $f(p)$ at point $p \in S$ is the least distance of p to the medial axis.

A geodesic disk $B(p, r)$ centered at p with radius r is the the point sets

$$B(p, r) = \{q \in S \mid d(p, q) \leq r\},$$

d is the geodesic distance on the surface. The *injectivity radius* at a point $p \in S$ is the largest radius $\tau(p)$, for which the geodesic disk $B(p, \tau(p))$ is an embedding on S .

Suppose $\epsilon : S \rightarrow R$ is a positive function defined on the surface S , a point set X is an ϵ -*sample*, if for any point $p \in S$, there is at least one sample inside the geodesic disk $B(p, \epsilon(p))$.

The definition of Delaunay triangulations of X on S is the same as it is in R^2 . They are defined as having the empty circumscribing circle property: the circum-circle for each geodesic triangle contains no vertices of the triangulation in its interior. In order to gurantee the uniqueness and embedness of the circum-circles, X should be dense enough.

Leibon et al. proved in [LL00] that, suppose X is a generic ϵ -sample, ϵ satisfies the following conditions:

$$\epsilon(p) \leq \min\left\{\frac{2\tau(p)}{5}, \frac{2\pi}{5k(p)}\right\}, \quad (1)$$

where $k(p) = \max_{q \in B(p, \tau(p))} |k(q)|$, then the delaunay triangulation of X exists and is unique.

2.2 Hausdorff Distance, Normal Distance and the Nearest Distance Map

Let $M_1, M_2 \subset R^3$ be non empty point sets, the *Hausdorff distance* between M_1 and M_2 is defined as

$$d_H(M_1, M_2) = \inf\{\epsilon > 0 | M_1 \subset U_\epsilon(M_2), M_2 \subset U_\epsilon(M_1)\}, \quad (2)$$

where $U_\epsilon(M) = \{x \in R^3 | \exists y \in M : d(x, y) < \epsilon\}$.

Suppose S and M are two surfaces embedded in R^3 , the shortest distance map $g : M \rightarrow S$ is defined to map $p \in M$ to its nearest point $g(p)$ on S . It is proved that the line connecting p to $g(p)$ is along the normal direction at $g(p)$ on S . It has been proven in [LL00], if the sample density ϵ satisfies 2 and the following

$$\epsilon(p) \leq \frac{f(p)}{4}, \quad (3)$$

then the g is a homeomorphism between the mesh M and S induced by the Delaunay triangulation. Then we denote the inverse of g as $\Phi = g^{-1} : S \rightarrow M$, then

$$\Phi(p) = p + \phi(p)\mathbf{n}(p), p \in S \quad (4)$$

where $\mathbf{n}(p)$ is the normal vector at p on S , $\phi(p)$ measures the distance from p to $\Phi(p)$ on the mesh. The normal distance between S and M is defined as

$$d_n(S, M) = \max_{p \in S} |\mathbf{n}(p) - \mathbf{n} \circ \Phi(p)|.$$

Suppose $\gamma : t \rightarrow S$ is a curve on S , then $\Phi \circ \gamma : t \rightarrow M$ is a curve on M . It is proven in [HPW05], the infinitesimal distortion of length satisfies

$$\min_i (1 - \phi k_i) \leq \frac{dl_M}{dl} \leq \frac{1 - \phi k_i}{\langle \mathbf{n}, \mathbf{n} \circ \Phi \rangle}, \quad (5)$$

where $dl = \sqrt{\langle d\gamma, d\gamma \rangle}$ is the length element on S , $dl_M = \sqrt{\langle d\gamma \circ \Phi, d\gamma \circ \Phi \rangle}$ is the corresponding length element on M , k_i is the principle curvature.

3 Geometric Accuracy Analysis

In this section, we analyze the geometric accuracy of reconstructed meshes. Suppose X is an ϵ -sample on S , if ϵ is small enough then X induces a unique Delaunay triangulation T , where all edges are geodesics. Each face on T has a unique geodesic circumscribed circle, the bound of all the radii is $r(X)$ determined the sampling density ϵ . Then by replacing geodesic triangles on T to Euclidean triangles, a piecewise linear complex $M(X)$ is produced, denoted as the *Delaunay mesh* induced by X . Our goal is to estimate the Hausdorff error, normal error and metric error between S and M , in terms of the $r(X)$ and sampling density ϵ .

The following is the major steps of our proof,

1. We first estimate the Hausdorff distance between a geodesic triangle and the planar triangle through its vertices.
2. Then we estimate the normal deviation between the normal at an arbitrary point in a geodesic triangle and the normal of the planar triangle.
3. Finally we discuss the Hausdorff distance and normal distance between S and M , then we estimate the metric distortion.

3.1 Hausdorff Distance Between a geodesic triangle and a planar triangle

Lemma 0.1 *Let $R(t)$ be an arc length parameterized smooth space curve with curvature bound $\kappa > 0$, $0 \leq a, b, t, t' \leq \pi/\kappa$, $\vec{m} = \frac{R(b)-R(a)}{|R(b)-R(a)|}$ then the following estimates hold*

$$t \geq |R(t)| > 2 \sin(\kappa t/2)/\kappa \quad (6)$$

$$|R'(t) \times \vec{m}| \leq \frac{1}{4} \kappa (b-a), \quad t \in [a, b], \kappa(b-a) < \sqrt{6} \quad (7)$$

$$|R'(t') - R'(t)| \leq |2 \sin(\kappa(t-t'))| \quad (8)$$

$$\angle R(a)R(t)R(b) \geq \pi/2 \quad (9)$$

$$|R'(t) \times \vec{m}| \leq \frac{\kappa(b-a) \min(t-a, b-t)}{4}, \quad 0 < a < t < b < \sqrt{6}/\kappa \quad (10)$$

$$0 < (R(t) - R(a), \vec{m}) < |R(b) - R(a)|, \quad t \in (a, b) \quad (11)$$

where $\text{dist}(\cdot, \cdot)$ denote the distance.

Proof: Consider function $f(t) = (R'(t), R'(0))$, then since $R'(t) \perp R''(t)$,

$$\begin{aligned} f'(t) &= (R''(t), R'(t_0)) = (R''(t), R'(t_0) - (R'(t_0), R'(t))R'(t)) \\ &\geq -\kappa |R'(t) \times R'(t_0)| = -\kappa \sqrt{1 - f^2(t)} \end{aligned}$$

$f(t)$ satisfies $f'(t) \geq -\kappa \sqrt{1 - f^2(t)}$, then

$$\begin{aligned} \frac{\partial}{\partial t} (\arccos f(t)) &\leq \kappa \\ f(t) &\geq \cos(\kappa t), \quad t \in [0, \pi/\kappa] \end{aligned}$$

Now the estimates follows by integration:

$$\begin{aligned} |R(t)|^2 &= \int_0^t \int_0^t (R'(t_1), R'(t_2)) dt_1 dt_2 \\ &\geq \int_0^t \int_0^t \cos(\kappa(t_2 - t_1)) dt_1 dt_2 \\ &= 4\kappa^{-2} \sin^2(\kappa t/2) \Rightarrow (6) \end{aligned}$$

$$\begin{aligned}
|R(b) - R(a)|(R'(t), \vec{m}) &\geq \int_a^b \cos \kappa(s-t) ds \\
&= \frac{1}{\kappa} (\sin \kappa(b-t) + \sin \kappa(t-a)) \quad (12) \\
&\geq (b-a) - \frac{\kappa^2(b-a)^3}{6} \\
|R'(t) \times \vec{m}| &= \sqrt{1 - (R'(t), \vec{m})^2} \\
&\leq \sqrt{1 - (1 - \kappa^2(b-a)^2/6)^2}, \quad \text{if } (b-a) < \sqrt{6} \\
&\leq \frac{\sqrt{2}}{6} \kappa(b-a) \Rightarrow (7)
\end{aligned}$$

Equation (12) implies $(R'(t), R(b) - R(a)) > 0$ when $b-a < \pi$, hence $(R(t), R(b) - R(a))$ is an increasing function of t , hence (11) is proved.

$$\begin{aligned}
(R(b) - R(t), R(t) - R(a)) &\geq \int_a^t \int_t^b \cos \kappa(u-v) dudv \\
&= \cos \kappa(b-t) + \cos \kappa(t-a) - 1 - \cos(b-a) \\
&\geq 0, \quad \text{if } \kappa(b-a) < \pi \Rightarrow (9).
\end{aligned}$$

$$(R'(t), R'(t')) \geq \cos \kappa(t' - t), \quad |R(t)| = |R'(t)| = 1 \Rightarrow (8)$$

Assume $t-a < b-t$, then (7) implies that

$$\text{dist}(R(t), R(a)R(b)) = |(R(t) - R(a)) \times \vec{m}| \leq \kappa(b-a)(t-a)/4 \Rightarrow \text{Eqn}(10).$$

□

Notation: We use $\widetilde{}$ to denote an geometric object on a surface in geodesic sense, such as \widetilde{AB} , $\widetilde{\Delta ABC}$ to denote a geodesic or a geodesic triangle.

Lemma 0.2 *P, Q are two points in a geodesic convex region of a smooth surface with principal curvature bounded by κ , then the normal at P, Q differs by at most $\kappa|\widetilde{PQ}|$.*

Proof: Bound of principal curvature implies $|\nabla \vec{n}| \leq \kappa$, where ∇ is the covariant derivative and \vec{n} is the normal. Hence the estimate. □

The following theorem estimate the distance of points inside a geodesic triangle to the plane through the vertices, independent of the shape of the triangle.

Theorem 1 *Let $\widetilde{\Delta ABC}$ be a geodesic triangle on a smooth surface embedded in \mathbb{R}^3 where the principal curvature is bounded by κ and the maximal length d of edges of $\widetilde{\Delta ABC}$ is bounded by $1/\kappa$. P is any point inside the triangle, P_{ABC} is the plane through A, B, C , then the $\text{dist}(P, P_{ABC}) \leq \kappa d^2/4$.*

Proof: Assume A is the vertex farthest from P , \widetilde{AP} intersects \widetilde{BC} at Q , P' is the projection of P onto AQ . By (10),

$$\begin{aligned}
\text{dist}(Q, P_{ABC}) &\leq \text{dist}(Q, BC) \leq \kappa d^2/8. \\
|PP'| &\leq \kappa d^2/8
\end{aligned}$$

(11) implies that P' is inside AQ and $\text{dist}(P', P_{ABC}) \leq \text{dist}(Q, P_{ABC})$,

$$\text{dist}(P, P_{ABC}) \leq |PP'| + \text{dist}(P', P_{ABC}) \leq \kappa d^2/4$$

□

3.2 Normal Error Estimation between a geodesic triangle and a planar triangle

Lemma 1.1 *Let \widetilde{ABC} be a geodesic triangle with maximal length of edge d , the principal curvature is bounded by κ , $d < 2/\kappa$, $\angle BAC = \alpha$, then the normal n_A to the surface at A and the normal n to P_{ABC} satisfies*

$$|n_A \times n| \leq \max\left(\frac{\kappa d}{4 \sin(\alpha/2)}, \frac{\kappa d}{4 \cos(\alpha/2)}\right) \quad (13)$$

Proof: Denote by T_1 the tangent vector at A to \widetilde{AB} , T_2 tangent to \widetilde{AC} , V_1 the unit vector along AB , V_2 along AC . Then by (7)

$$|T_1 \times V_1| \leq \kappa d/2, |T_2 \times V_2| \leq \kappa d/4$$

So

$$\begin{aligned} |(n_A, V_1)| &= |(n_A, V_1 - (V_1, T_1)T_1)| \\ &\leq |V_1 - (V_1, T_1)T_1| = |T_1 \times V_1| \leq \kappa d/4 \\ |(n_A, V_2)| &\leq \kappa d/4 \end{aligned}$$

The projection of n_A onto P_{ABC} falls into the parallelogram with both width $\kappa d/2$ and inner angle $\alpha, \pi - \alpha$, centered at A . Now (13) follows by simple trigonometry. □

Lemma 1.2 *Let $l(t)$ be a geodesic circle radius r , parameterized by arc length. Suppose the principal curvature is bounded by κ in the disk and $r \leq 1/(4\kappa)$. $N(t)$ is the tangent vector at $l(t)$ normal to $l'(t)$. Then for $t < r$,*

$$(l(t) - l(0), N(0)) \geq \frac{t^2}{5r} \quad (14)$$

Proof: Let $n(t)$ be the normal to the surface at $l(t)$. The curvature condition implies $|(l''(t), n(t))| \leq \kappa$. Hessian comparison theorem [SY94] implies

$$\begin{aligned} (l''(t), N(t)) &\geq \kappa \cot(\kappa r) \geq \frac{19}{20r}, \quad \text{if } \kappa r < 1/4 \\ |l''(t)| &\leq \kappa \sqrt{\coth \kappa r^2 + 1} \leq \frac{11}{10r}, \quad \text{if } \kappa r < 1/4 \end{aligned} \quad (15)$$

Lemma 1.1 implies $|n(t) - n(0)| \leq \kappa t$. (8) and (15) implies $|l'(t) - l'(0)| \leq 11t/10r$, then for $t \leq r$

$$\begin{aligned}
(l''(t), N(0)) &= (l''(t), N(t)) + (l''(t), N(0) - N(t)) \\
&= (l''(t), N(t)) + (l''(t), n(0) \times l'(0) - n(t) \times l'(t)) \\
&\geq (l''(t), N(t)) - |l''(t)|(|n(0) - n(t)| + |l'(0) - l'(t)|) \\
&\geq \frac{1}{r} \left(\frac{19}{20} - \frac{11\kappa t}{10} - \frac{121t}{100r} \right)
\end{aligned} \tag{16}$$

Use $l'(0) \perp N(0)$, integrate (16) to get

$$(l(t) - l(0), N(0)) \geq \frac{9t^2}{40r}$$

□

Theorem 2 *D is a geodesic disk of radius r of a smooth surface embedded in \mathbb{R}^3 with principal curvature bounded by κ , $r < 1/(4\kappa)$. A, B, C are three distinct points on the boundary of D, P_{ABC} is the plane through A, B, C, ϕ is the projection map from D onto P_{ABC} . For any point $p \in D$, $v \in T_p$ is a tangent vector, we have*

$$|n_p - n_{ABC}| \leq 4.5\kappa r \tag{17}$$

$$|v| \geq |\phi_*(v)| \geq |v|(1 - 4.5\kappa r) \tag{18}$$

$$\text{dist}(p, P_{ABC}) \leq 9\kappa r^2 \tag{19}$$

Proof: Consider the intersection angle between the radial geodesic connecting center O of D and the vertices A, B, C .

If two such intersection angle is less than $9/10$, say $\angle AOB, \angle BOC$, then comparison theorem shows that the arc between A, B or between B, C along boundary of D is less than

$$\frac{9}{10} \cdot \frac{e^{\kappa r} - e^{-\kappa r}}{2\kappa} \leq r \tag{20}$$

Let d_1, d_2 be the length of line segment AB, BC respectively, then (11) implies $\angle ABC > \pi/2$ while Lemma 1.2 implies

$$\angle ABC \leq \pi - \arcsin(d_1/5r) - \arcsin(d_2/5r)$$

Then apply Lemma 1.1 to get

$$|n_B - n_{ABC}| \leq \frac{\kappa(d_1 + d_2)}{4 \cos(\angle ABC)/2} \leq \frac{\kappa(d_1 + d_2)}{2d_1/5r + 2d_2/5r} = 2.5\kappa r$$

If only one such intersection angle is less than $9/10$, say $\widetilde{\angle AOB}$. For the triangle AOC , by (6) and (7)

$$\begin{aligned}\angle AOC &\geq 9/10 - 2 \arcsin(\kappa r/4) \geq 0.77 \\ r &> |OA|, |OC| > .99r\end{aligned}$$

$$|AC| \geq 2 * .99 \sin(0.77/2)r > 0.74r \quad (21)$$

$$\angle CAO \leq \arccos((.99^2 + .74^2 - 1)/(2 * .99 * .74)) < 1.21$$

$$\angle BAO \leq \pi/2 + \arcsin(\kappa r/4) \leq 1.64$$

$$4 \cos(\angle(CAB)/2) \geq 4 \cos(1.425) \geq 0.58 \quad (22)$$

On the other hand for $\triangle ABC$, $r > |AC|, |BC| \geq 0.74r$ by (21), $|AB| \leq r$ by (20), so

$$\begin{aligned}\angle BAC &\geq \min(\arccos(.5/.74), 2 \arcsin(.74/2)) \geq .75 \\ 4 \sin(\angle BAC/2) &\geq 1.4\end{aligned} \quad (23)$$

Now apply Lemma 1.1 with estimate (22) and (23) to give an estimate of the difference of the normal at A and to the plane ABC , then use Lemma 0.2 to get (17).

Given (17) proved, (18) easily follows as

$$|v - \phi_*(v)| = |(v, n_{ABC})| = |(v, n_{ABC} - n_A)| \leq 4.5\kappa r|v|$$

and for (19), let $l(t)$ be the geodesic connecting A and p

$$\text{dist}(p, P_{ABC}) = \left| \int_l (l'(t), n_{ABC}) dt \right| \leq \widetilde{\text{dist}}(p, A) * 4.5\kappa r \leq 9\kappa r^2$$

□

3.3 Geometric Accuracy for Delaunay Meshes

Combine the theoretic results in section 2 and the estimations on a single geodesic triangle theorem 1 and theorem 2, we can easily get the following theorem.

Theorem 3 *Suppose S is a closed C^2 smooth surface embedded in R^3 . The principle curvature upper bound is k , the injective radius lower bound is τ , the lower bound of local feature size is f . Suppose X is a ϵ -sample set on S , such that constant ϵ satisfies the following conditions,*

$$\epsilon \leq \min\left\{\frac{2\tau}{5}, \frac{2\pi}{5k}, \frac{f}{4}, \frac{1}{4k}\right\},$$

then X induces a unique Delaunay triangulation T , (X, T) induces a piecewise linear complex M ,

1. M is homeomorphic to S , the nearest distance map $\Phi : M \rightarrow S$ is a homeomorphism.

2. *The Hausdorff distance*

$$d_H(M, S) \leq 4k\epsilon^2 \quad (24)$$

3. *The normal distance*

$$d_n(M, S) \leq 9k\epsilon \quad (25)$$

4. *The infinitesimal length ratio*

$$1 - 4k^2\epsilon^2 \leq \frac{dl_M}{dl} \leq \frac{1 + 4k^2\epsilon^2}{1 - 9k\epsilon}. \quad (26)$$

Proof: Because X is an ϵ -sample, ϵ satisfies the condition in 2, therefore the unique Delaunay triangulation T exists from [LL00]. ϵ is less than a quarter of the local feature size 3, then the nearest distance map is a homeomorphism.

Suppose C is a circumscribe circle of a triangle in T , then there is no interior point belonging to X . If the radius of C is greater than 2ϵ , then C contains at least disks with radii ϵ , therefore, it contains at least one point of X as its interior. Thus the radius of C is no greater than 2ϵ .

From theorem 1, the Hausdorff distance is no greater than $4k\epsilon^2$. From theorem 2, the normal distance is no greater than $9k\epsilon$.

In the nearest distance map 4, ϕ is less or equal to the Hausdorff distance. From formula 5 we can derive the 26. \square

Although the sample density ϵ is a constant here, it can be generalized to be a function on the surface, such that

$$\epsilon(p) \leq \min\left\{\frac{2\tau(p)}{5}, \frac{2\pi}{5k(p)}, \frac{f(p)}{4}, \frac{1}{4k(p)}\right\},$$

then we can estimate the Hausdorff distance, normal distance and metric distortion at point p using the formula similar to 24,25,26 with ϵ replaced by $\epsilon(p)$.

4 Experimental Results

In order to verify our theorems, we tessellate several smooth surfaces with different resolutions, and measure the Hausdorff distance and normal deviation.

The smooth surfaces are represented as NURBS surfaces, therefore the computation of the bound of principle curvature is straight forward.

The Hausdorff distance is calculated by minimizing the following functional, suppose $p \in M$, S is $S(u, v)$

$$f(u, v) = \langle S(u, v) - p, S(u, v) - p \rangle.$$

For any point p on M , first we find the closest vertex p_0 on M , p_0 is also on S with parameter (u_0, v_0) . Then we use (u_0, v_0) as the initial point, then use Newton's method to find the global minimum of $f(u, v)$. We densely sample M , and find the maximum distance between the sample points to S .

Table 4 illustrates the numerical results. From the table it is obvious that our theoretic estimated Hausdorff errors converge to the real measured Hausdorff error when the sampling density is increased. This verifies our theoretic results.

Shape	Vertices	Edges	D	κ	d	$1/4\kappa d^2$
sphere	92	180	0.013750	1.758418	3.420931	0.656359
sphere	252	500	0.010597	1.758418	1.248911	0.135940
sphere	1002	2000	0.010025	1.758418	0.314097	0.014678
torus	60	120	0.153249	4.525904	2.467277	0.839321
torus	120	240	0.051237	4.525904	1.233638	0.216549
torus	240	480	0.049931	4.525904	0.616819	0.065040
knot	400	800	0.039319	9.280646	1.955026	0.215511
knot	840	1680	0.035839	9.280646	0.930965	0.111673
knot	2000	4000	0.032552	9.280646	0.391005	0.053959
teapot	302	552	0.040195	1104.996852	2.293478	2.381761
teapot	822	1560	0.021245	1104.996852	0.842616	0.809765
teapot	3242	6320	0.020297	1104.996852	0.213643	0.196828

Table 1: D the real Hausdorff distance measured. κ maximal principal curvature. d maximal length of edges. $1/4\kappa d^2$ maximum of the estimated distance.

5 Conclusion and Future Work

This work gives explicit formula of approximation error bounds for both Hausdorff distance and normal distance in terms of sampling density. For a set of sample points on a surface with sufficient density, it induces a unique Delaunay triangulation, and a discrete mesh. With the increase of sampling density, the Delaunay meshes converge to the original surface under both Hausdorff distance and normal distance, therefore, the area, the Riemannian metrics and the Laplace-Beltrami operators are also convergent.

In the future, we will apply these error estimation formula to prove the convergence of other advanced algorithms in geometric modeling and processing, such as the conformal parameterizations, Poisson editing etc.

References

- [AB99] Nina Amenta and Marshall W. Bern. Surface reconstruction by voronoi filtering. *Discrete & Computational Geometry*, 22(4):481–504, 1999.
- [ABK98] Nina Amenta, Marshall W. Bern, and Manolis Kamvysselis. A new voronoi-based surface reconstruction algorithm. In *SIGGRAPH*, pages 415–421, 1998.
- [ACDL02] Nina Amenta, Sunghee Choi, Tamal K. Dey, and N. Leekha. A simple algorithm for homeomorphic surface reconstruction. *Int. J. Comput. Geometry Appl.*, 12(1-2):125–141, 2002.
- [BB97] Fausto Bernardini and Chandrajit L. Bajaj. Sampling and reconstructing manifolds using alpha-shapes. In *CCCG*, 1997.

- [BBX95] Chandrajit L. Bajaj, Fausto Bernardini, and Guoliang Xu. Automatic reconstruction of surfaces and scalar fields from 3d scans. In *SIGGRAPH*, pages 109–118, 1995.
- [BCG05] Mirela Ben-Chen and Craig Gotsman. On the optimality of spectral compression of mesh data. *ACM Trans. Graph.*, 24(1):60–80, 2005.
- [BMV01] Pál Benkő, Ralph R. Martin, and Tamás Várady. Algorithms for reverse engineering boundary representation models. *Computer-Aided Design*, 33(11):839–851, 2001.
- [EH96] Matthias Eck and Hugues Hoppe. Automatic reconstruction of b-spline surfaces of arbitrary topological type. In *SIGGRAPH*, pages 325–334, 1996.
- [Fed59] Herbert Federer. Curvature measures. *Transactions of the American Mathematical Society*, 93:418–491, 1959.
- [FH05] Michael S. Floater and Kai Hormann. Surface parameterization: a tutorial and survey. In N. A. Dodgson, M. S. Floater, and M. A. Sabin, editors, *Advances in multiresolution for geometric modelling*, pages 157–186. Springer Verlag, 2005.
- [FR01] Michael S. Floater and Martin Reimers. Meshless parameterization and surface reconstruction. *Computer Aided Geometric Design*, 18(2):77–92, 2001.
- [HDD⁺92] Hugues Hoppe, Tony DeRose, Tom Duchamp, John Alan McDonald, and Werner Stuetzle. Surface reconstruction from unorganized points. In *SIGGRAPH*, pages 71–78, 1992.
- [Hop96] Hugues Hoppe. Progressive meshes. In *SIGGRAPH*, pages 99–108, 1996.
- [HPW05] Klaus Hildebrandt, Konrad Polthier, and Max Wardetzky. On the convergence of metric and geometric properties of polyhedral surfaces. 2005. submitted.
- [HQ04] Ying He and Hong Qin. Surface reconstruction with triangular b-splines. In *GMP*, pages 279–290, 2004.
- [JLSW02] Tao Ju, Frank Losasso, Scott Schaefer, and Joe D. Warren. Dual contouring of hermite data. In *SIGGRAPH*, pages 339–346, 2002.
- [LL00] Greg Leibon and David Letscher. Delaunay triangulations and voronoi diagrams for riemannian manifolds. In *Symposium on Computational Geometry*, pages 341–349, 2000.
- [SSK⁺05] Vitaly Surazhsky, Tatiana Surazhsky, Danil Kirsanov, Steven J. Gortler, and Hugues Hoppe. Fast exact and approximate geodesics on meshes. *ACM Trans. Graph.*, 24(3):553–560, 2005.

- [SY94] Richard Schoen and Shing-Tung Yau. *Lectures on Differential Geometry*. International Press, Cambridge, MA, 1994.

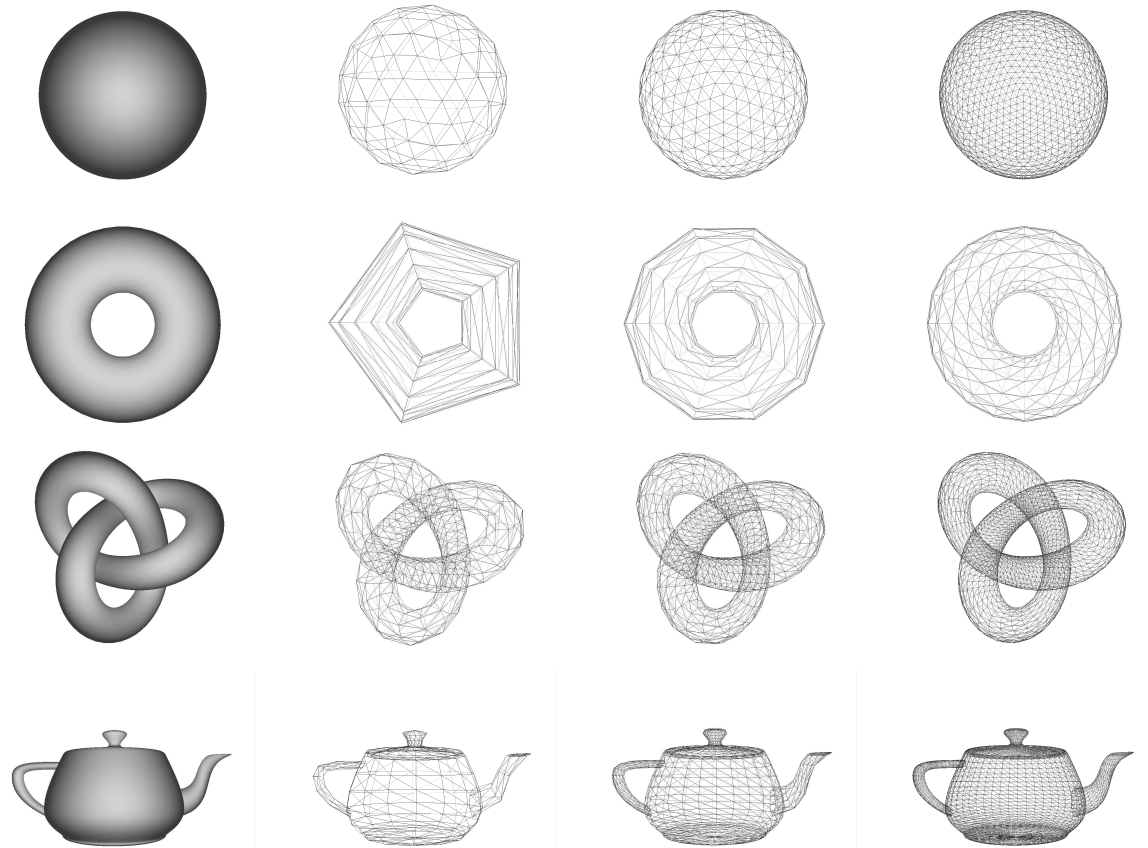


Figure 3: Smooth surfaces approximated meshes, which are induced by Delaunay triangulations with different sampling density.